

RESEARCH ARTICLE

Application of Permeability-Limited Physiologically-Based Pharmacokinetic Models: Part I–Digoxin Pharmacokinetics Incorporating P-Glycoprotein-Mediated Efflux

SIBYLLE NEUHOFF,¹ KAREN ROWLAND YEO,¹ ZOE BARTER,¹ MASOUD JAMEI,¹ DAVID B. TURNER,¹ AMIN ROSTAMI-HODJEGAN^{1,2}

¹Simcyp Limited (a Certara company), Blades Enterprise Centre, John Street, Sheffield S2 4SU, UK

²School of Pharmacy and Pharmaceutical Sciences, Faculty of Medical and Human Sciences, University of Manchester Stopford Building Oxford Road, Manchester M13 9PT, UK

Received 25 March 2013; revised 16 April 2013; accepted 17 April 2013

Published online in Wiley Online Library (wileyonlinelibrary.com). DOI 10.1002/jps.23594

ABSTRACT: A prerequisite for the prediction of the magnitude of P-glycoprotein (P-gp)-mediated drug–drug interactions between digoxin and P-gp inhibitors (*e.g.* verapamil and its metabolite norverapamil) or P-gp inducers (*e.g.* rifampicin) is a predictive pharmacokinetic model for digoxin itself. Thus, relevant *in vitro* metabolic, transporter and inhibitory data incorporated into permeability-limited models, such as the “advanced dissolution, absorption and metabolism” (ADAM) module and the permeability-limited liver (PerL) module, integrated with a mechanistic physiologically-based pharmacokinetic (PBPK) model such as that of the Simcyp Simulator (version 12.2) are necessary. Simulated concentration–time profiles of digoxin generated using the developed model were consistent with observed data across 31 independent studies [13 intravenous single dose (SD), 12 per oral SD and six multiple dose studies]. The fact that predicted t_{\max} (time of maximum plasma concentration observed) and C_{\max} (maximum plasma concentration observed) of oral digoxin were similar to observed values indicated that the relative contributions of permeation and P-gp-mediated efflux in the model were appropriate. There was no indication of departure from dose proportionality over the dose range studied (0.25–1.5 mg). All dose normalised area under the plasma concentration–time curve profiles (AUCs) for the 0.25, 0.5, 0.75 and 1 mg doses resembled each other. Thus, PBPK modelling in conjunction with mechanistic absorption and distribution models and reliable *in vitro* transporter data can be used to assess the impact of dose on P-gp-mediated efflux (or otherwise). © 2013 Wiley Periodicals, Inc. and the American Pharmacists Association J Pharm Sci

Keywords: P-glycoprotein; ABCB1; MDR1; simulation; digoxin; IVIVE; pharmacokinetics; transporter

INTRODUCTION

P-glycoprotein (P-gp) is a well-characterised adenosine triphosphate (ATP) binding cassette (ABC) transporter of the multidrug resistance and transporter associated with antigen processing (MDR/TAP) subfamily. P-gp is extensively distributed and expressed in the luminal membrane of the intestinal epithelium, capillary endothelial cells such as the

blood–brain barrier and in drug-eliminating organs, including the liver, that is, within the canalicular membrane of hepatocytes, and kidney, that is, within the apical membrane of proximal tubule cells.¹ The expression of P-gp in these tissues is related to its role in the excretion of substances into the gut lumen, the bile and the urine. The extensive tissue distribution and the wide variety of therapeutically relevant compounds transported by P-gp clearly indicate its important role in drug absorption, distribution and elimination. It has been demonstrated that modulation of the expression and/or activity of P-gp due to genetic or environmental factors may have a significant impact on drug disposition, drug effectiveness or drug toxicity.

Additional Supporting Information may be found in the online version of this article. Supporting Information

Correspondence to: Sibylle Neuhoff (Telephone: +44-114-292-2325; Fax: +44-114-292-2222; E-mail: S.Neuhoff@simcyp.com)

Journal of Pharmaceutical Sciences

© 2013 Wiley Periodicals, Inc. and the American Pharmacists Association

Digoxin has been identified as a substrate of P-gp and is mainly excreted unchanged via the kidneys.^{2,3} *In vitro* and animal experiments have demonstrated the importance of both renal and intestinal P-gp in the disposition of digoxin.^{2,4,5} Due to the narrow therapeutic window of digoxin, relatively small increases in exposure have been associated with serious adverse reactions.^{6,7} Thus, close monitoring of digoxin serum levels is advocated.

We have previously investigated the interplay between metabolism and transport in the gut using the advanced dissolution, absorption and metabolism (ADAM) model⁸ to assess the key determinants of oral drug absorption and gut wall metabolism within common physicochemical and biological parameter spaces for small molecule drugs.⁹ We now present application of the model to a specific case, namely digoxin, which

has a clinical dose range of 0.25–1.5 mg, and demonstrate the validity and benefits of using a mechanistic physiologically-based pharmacokinetic (PBPK) model that incorporates both permeability-limited liver (PerL) and gut (ADAM) modules; the latter considers regional differences in permeability and P-gp-mediated efflux along the intestine.¹⁰

METHODS

A workflow describing the model building and validation processes that were applied to the development of the digoxin PBPK model is outlined in Figure 1. This follows some of the recommendations and outline given by Zhao *et al.* (2012).¹¹ A general schematic representation of the PBPK models applied in this study

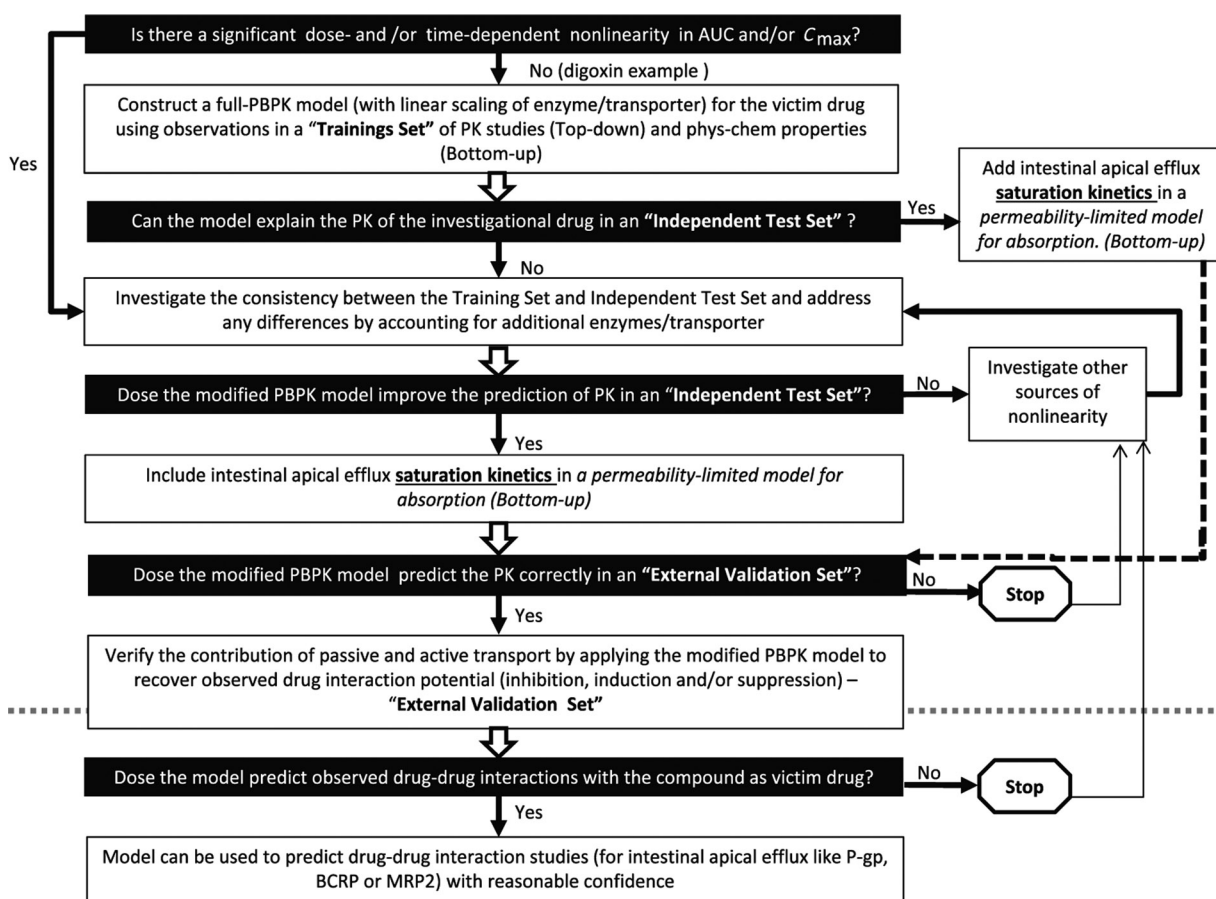


Figure 1. Applied workflow for a victim drug (digoxin) to address intestinal apical efflux, which is non-saturable by the victim, but inhibitable by other drugs, that is, perpetrators, using PK data and PBPK modelling and simulations. The training set is a set of data from clinically observed investigations used to derive some of the kinetic parameters under certain study design and dosage regimen. The independent test set is a set of data obtained from similar type of studies to those conducted in the protocol of the training set. The external validation set is a set of data that evaluated the performance of the model independent of the trainings and test sets. AUC, area under the concentration–time curve; PK, pharmacokinetic; PBPK, physiologically-based pharmacokinetic; P-gp, P-glycoprotein; BCRP, breast cancer resistant protein; MRP2, multidrug-resistance related protein 2

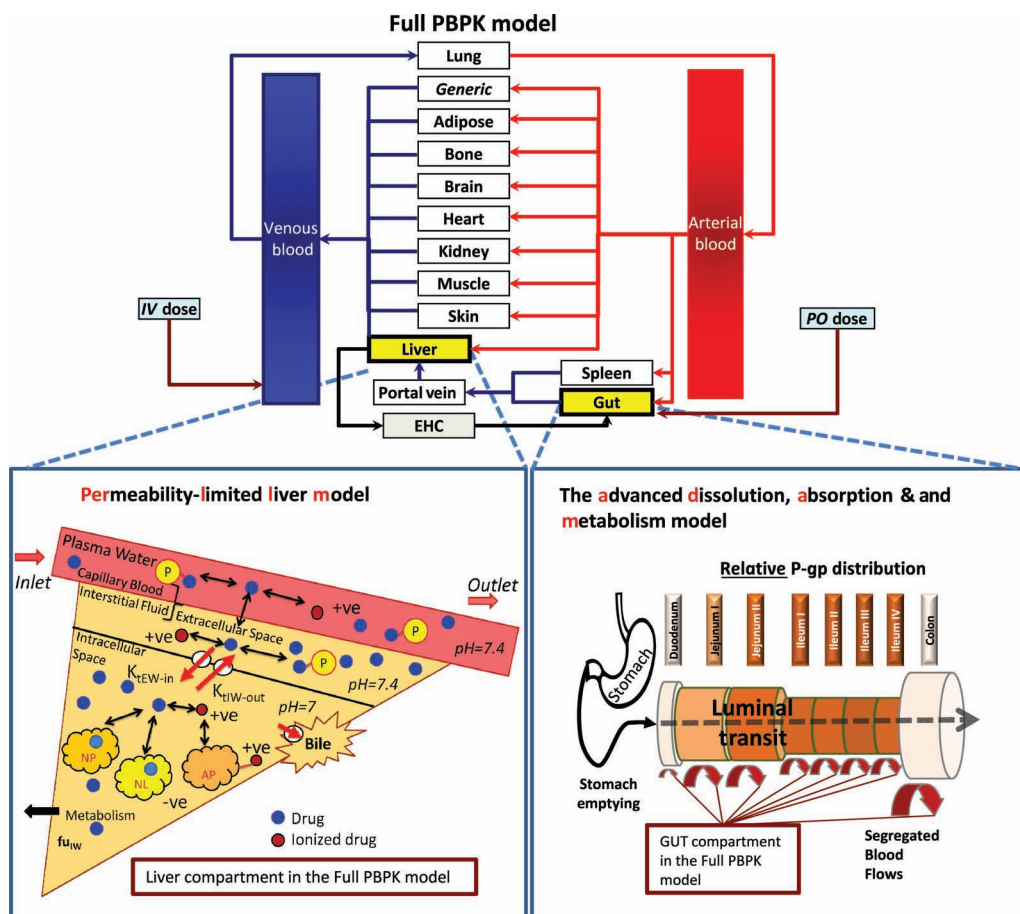


Figure 2. PBPK models used for describing the kinetics of digoxin. The absorption of digoxin after oral administration was described by the ADAM model. The ADAM module represents the GI tract as compartments based upon their physiological and anatomical attributes hence the relationship between permeability, metabolism and dissolution, amongst other factors, can be assessed quantitatively. Once the drug has passed into the portal vein the kinetics of digoxin were described by a full PBPK model assuming permeability-limited diffusion into the liver (PerL).

is shown in Figure 2. A description of the sub-models and the sources of information are provided below.

Sub-Models Contributing to the Digoxin PBPK Model

To account for transporter kinetics, the absorption of digoxin after oral administration was described by the ADAM model, which divides the gastrointestinal (GI) tract into nine segments.^{8,12} In the ADAM model, these segments are heterogeneous with respect to size, abundance of enzymes and transporters, transit time, pH and bile salt concentration.¹³ Because the ADAM module represents the GI tract as compartments based upon their physiological and anatomical attributes (Fig. 2), the relationship between permeability, metabolism and dissolution, amongst other factors, can be considered quantitatively. The model incorporates fluid dynamics which is necessary for mechanistic modelling of oral drug absorption following release from formulation, dissolution, precipita-

tion, super-saturation, luminal degradation, permeability, metabolism, active transport and the transit between GI segments. The blood flows to each anatomical region of the GI tract are defined separately and metabolism and transport are considered independently in each intestinal compartment. Thus, the model has features in common with the segmental segregated flow model described by Tam and co-workers¹⁴ at the University of Toronto.¹⁵ It is assumed that each enterocyte is a well-stirred cell where efflux transporters (*e.g.* P-gp, BCRP and MRP2) and intestinal enzymes compete for binding to the substrate.

Once the drug has passed into the portal vein the kinetics of digoxin are described by a full PBPK model assuming permeability-limited diffusion into the liver¹⁶ (Fig. 2). The volume of distribution (V_{ss}) was predicted using the method reported by Rodgers and co-workers.^{17–19} A number of tissue–plasma partition coefficients ($P_{t,p}$) in human were available in the

Table 1. Parameter Values Used for the Digoxin Simulations

| Parameter | Value | Reference/Comments |
|---|-----------|---|
| Dose (mg) | 0.5 | |
| MW (g/mol) | 780.94 | |
| fu-experimental | 0.71 | Meta-analysis ^{26–29} |
| C _B /C _P -experimental | 1.07 | Refs.28,30 |
| log P-experimental | 1.26 | Refs. 3,37,27 |
| Compound type | Neutral | Within the physiological pH range |
| Absorption | | |
| Model | ADAM | |
| P _{eff,man} (10 ⁻⁴ cm/s) | 0.1–4.67 | Predicted using the Mech P _{eff} model (see text for details) |
| fa-predicted | 0.82 | Based on Mech P _{eff} prediction |
| ka (h ⁻¹)-predicted | 0.59 | Based on Mech P _{eff} prediction |
| ka (h ⁻¹)-observed | 0.58–7.4 | Range from Refs. 2,33–36 |
| Distribution | | |
| Model | Full PBPK | |
| V _{ss} (L/kg)-predicted | 6.33 | Rodgers and Rowland method (see text for details) |
| V _{ss} (L/kg)-observed | 5.02 | Meta-analysis ^{3,37,27} |
| Kp muscle | 7.35 | Refs. 20–22,38 |
| Kp adipose | 10.8 | Ref. 20 |
| Elimination | | |
| CL _{iv} (L/h) | 13.46 | Meta-analysis ^{2,39–43} |
| Human hepatocyte CL _{int} (μL/min/million hepatocytes) | 0.37 | Calculated using the Retrograde model |
| CL _R (L/h) | 9.65 | Meta-analysis ^{2,3,27,37,39,40,43–45} |
| Transport (active and passive) | | |
| Intestinal efflux | | |
| J _{max} (pmol/min/cm ²) | 434 | Ref. 23 |
| K _{mu} (μM) | 177 | Ref. 23 |
| Intestinal P-gp REF for Caco-2 | 2 | Ref. 46 |
| Hepatic efflux | | |
| J _{max} (pmol/min/million hepatocytes) | 434 | Ref. 23; assuming that P-gp in 1 million hepatocytes have the same P-gp activity as the P-gp available in 1 cm ² of Caco-2 in the Transwell system |
| K _{mu} (μM) | 177 | Ref. 23 |
| Hepatic P-gp REF for Caco-2 | 1.5 | Scaled based on abundance relationship ^{47–50} |
| CL _{PD} (mL/min/million hepatocytes) | 0.1 | Default value, thus assuming a blood flow limited passive diffusion at the sinusoidal membrane, that is, indirectly accounting for active transport across the sinusoidal membrane of hepatocytes |

fa, the fraction of dose absorbed, *i.e.* entering the cellular space of the enterocytes from the gut lumen.

literature; values of 10.8²⁰ and 7.35^{21,22} were used for adipose and muscle, respectively, whereas the P_{t,p} values for the remaining tissues were predicted according to the Rodgers and Rowland method.^{18,19}

In the permeability-limited modules, transport-mediated gut absorption is described using Michaelis–Menten type equations (J_{\max} , maximum flux; K_m , substrate concentration giving half J_{\max}).^{23,24} In this model, the active and passive transport processes are considered separately and it is possible to investigate the impact of inhibitors and/or inducers on transporters individually or collectively. In the case of P-gp, J_{\max} and K_m values are generally obtained from transport experiments across Caco-2, MDCKII-MDR1 or LLC-PK₁-MDR1 cell monolayers.^{23–25} It is worth noting that the kinetic values can only be obtained correctly if the proper concentration is used.²⁵ The intrinsic transporter clearance (CL_{int,T}) is a concentration- and time-dependent variable. Although the intestinal

CL_{int,T} has units of μL/min, J_{\max} is in pmol/min (both normalised for the filter area, *i.e.* cm²) and K_m is in μM, the hepatic transporters have a CL_{int,T} in μL/min/million cells, J_{\max} in pmol/min/million cells and K_m in μM to allow scaling of the *in vitro* data to the corresponding organ.

Data Used for Simulations of Digoxin Pharmacokinetics

In vitro and pharmacokinetic parameters for digoxin were taken from the literature (Table 1), where data from more than one source were available for the same parameter, weighted means were calculated based on the number of observations reported.

Whole-Organ Metabolic Clearance

Digoxin undergoes only minor metabolism and thus enzyme kinetics for specific isoforms have not been characterised quantitatively *in vitro*. Therefore, a global value of net intrinsic hepatic clearance (CL_{int,H}) was back-calculated from *in vivo* clearance

($CL_{iv,B}$) using Eq. 1:

$$CL_{int,H} = \frac{Q_H \times CL_{H,B}}{fu_B \times (Q_H - CL_{H,B})} \quad (1)$$

where $fu_B = fu/(C_B/C_P)$ (; values were 0.71 and 1.07 for fu and C_B/C_P , respectively), Q_H is hepatic blood flow (82.5 L/h) and $CL_{H,B}$ is the hepatic metabolic clearance in blood (3.48 L/h) derived from $CL_{iv,B}$ (13.46 L/h) after subtraction of $CL_{R,B}$ (Table 1). The estimated net $CL_{int,H}$ of 5.47 L/h was divided by an average liver weight of 1649 g,⁵¹ a hepatocytes per gram of liver (HPGL) value of 117.5 millions of cells/g liver⁵² and corrected for the apparent passive diffusion clearance (CL_{PD}) of 0.1 mL/min/ 10^6 hepatocytes to obtain a value of 0.37 μ L/min/ 10^6 hepatocytes (Table 1).

Permeability Data

The estimation of the effective permeability in human ($P_{eff,man}$) for digoxin using the Mechanistic P_{eff} model and human physiology data was based on a log $P_{o:w}$ value of 1.26, neutral compound type (within the gut lumen physiological pH range) and villous morphology values suggested by Oliver *et al.* (1998).⁵³ Assuming an average bile salt concentration of 2.3 mM in the fasted state jejunum, a $P_{eff,man}$ value of 4.67×10^{-4} cm/s can be estimated for the *Jejunum I* segment. For the fed state the estimated $P_{eff,man}$ for the *Jejunum I* is slightly lower with 3.96×10^{-4} cm/s, based upon an assumed jejunal average bile salt concentration of 10 mM; transcellular, rather than paracellular, permeation provides the major route of absorption. The unstirred boundary layer (UBL) is not rate limiting as expected at the low log $P_{o:w}$ of 1.26, *i.e.* the transcellular permeability is not very high and there is a high free fraction (f_{UBL}) in the UBL even in the fed state [$f_{UBL} = 100\%$ where (bile) = 0; fasted (bile) $f_{UBL} = 94\%$, fed (bile) $f_{UBL} = 77\%$]. The reported $P_{eff,man}$ includes within it this free fraction scalar and accounts for most of the difference in the $P_{eff,man}$ values predicted above.

A performance evaluation of the Mechanistic P_{eff} model is given by Pade *et al.* (2011).⁵⁴ In brief, and for the purposes of this study only, the following parameters were used for the human physiology model: (a) villous height 600 μ m; (b) inter-villous distance 40 μ m and (c) villous diameter 100 μ m.⁵³ A jejunal Plicae circulares surface area expansion of threefold was applied and a villous surface area expansion of 12-fold (based upon the villous dimensions above) but reduced to 3.6 for the effective surface area available for a compound of this epithelial permeability (using the method described by Oliver *et al.* (1998)⁵³).

The $P_{eff,man}$ in the ileum can be scaled down by threefold relative to the jejunum, *i.e.* accounting for the gradual reduction in the Plicae moving towards the distal ileum where they are generally absent in

humans. Thus, a $P_{eff,man}$ in the ileum of 1.67×10^{-4} cm/s was assumed and the colon permeability was set to 0.1×10^{-4} cm/s.

Formulation Data

The aqueous equilibrium solubility of digoxin is 0.024 mg/mL,⁵⁵ which is low and in general requires consideration in a PBPK modelling approach. However, the formulations currently on the market (Table 2) sufficiently increase the solubility and the rate/extent of dissolution to allow a simplified model to be used which assumes that digoxin remains in solution at all times and is thus available for absorption.

In Vitro–In Vivo Extrapolation of Transporter Data

Intestinal Transporters

In vitro enzyme kinetic data for P-gp-mediated efflux of digoxin were available from the literature (Table 1). For Caco-2 data, J_{max} (gut) values (pmol/min) were scaled to whole organ values, using the following equations:

$$P_{app,Tran,n} = \frac{J_{max}(gut)}{A(K_m + fu_{gut}C_{ent,n})} \quad (2)$$

where the *in vitro* apparent active permeability per gut segment ($P_{app,Tran,n}$) is calculated from the J_{max} (gut) and K_m by accounting for the filter area of the *in vitro* system (A , cm²) and the concentration at the binding site of P-gp, that is, currently assumed as the enterocyte concentration, $C_{ent,n}$, in the n th segment. Because we assume that only the unbound drug will have access to the transporter binding site, the enterocyte concentration is corrected for the free fraction in the gut (fu_{gut}). A series of ordinary differential equations describe the dynamics of the amount of solid mass trapped in the formulation and not available for dissolution ($A_{F,n}$), the amount of solid mass available for dissolution ($A_{S,n}$), the amount of dissolved drug ($A_{D,n}$; Eqs. 3 and 4, respectively) and hence the drug concentration in the enterocyte ($C_{ent,n}$; Eq. 5).

$$\frac{dA_{S,n}}{dt} = -\frac{dA_{diss,n}}{dt} - k_{t,n}A_{S,n} + k_{t,n-1}A_{S,n-1} + \frac{dA_{F,n}}{dt} \quad (3)$$

$$\begin{aligned} \frac{dA_{D,n}}{dt} = & \frac{dA_{diss,n}}{dt} - (k_{deg,n} + k_{a,n} + k_{t,n})A_{D,n} \\ & + k_{t,n-1}A_{D,n-1} + CL_{int-T,n}fu_{gut}C_{ent,n} \end{aligned} \quad (4)$$

$$\begin{aligned} \frac{dC_{ent,n}}{dt} = & \frac{1}{V_{ent,n}} [k_{a,n}A_{D,n} - Q_{ent,n}C_{ent,n} \\ & - (CL_{int-G,n} + CL_{int-T,n})fu_{gut}C_{ent,n}] \end{aligned} \quad (5)$$

Table 2. PK Studies Used for Performance Verification

| PK Study No. | References | Dosing Regime | <i>n</i> | Female (%) | Age (Years) | Formulation |
|----------------------------|-------------|---|----------|------------|-------------|-----------------------|
| PK study 1 ^a | Ref. 3 | 0.5 mg SD i.v. (1 h infusion) | 9 | 0 | 25–37 | Lanitor |
| PK study 2 ^a | Ref. 37 | 0.5 mg SD i.v. (30 s bolus) | 12 | 0 | 22–34 | Lanitor |
| PK study 3 ^b | Ref. 56 | 0.75 mg SD i.v. (20 min infusion) | 6 | NG | NG | Not stated |
| PK study 4 ^a | Ref. 40 | 0.75 mg SD i.v. (30 s bolus) | 8 | 0 | NG | Lanoxin |
| PK study 5 ^a | Ref. 40 | 0.75 mg SD i.v. (1 h infusion) | 8 | 0 | NG | Lanoxin |
| PK study 6 ^a | Ref. 41 | 0.75 mg SD i.v. (4 min bolus) | 12 | 0 | 21–39 | Novodigal |
| PK study 7 ^b | Ref. 56 | 1 mg SD i.v. (20 min infusion) | 6 | NG | NG | Not stated |
| PK study 8 ^a | Ref. 2 | 1 mg SD i.v. (30 min infusion) | 8 | 0 | 21–37 | Lanitor |
| PK study 9 ^b | Ref. 57 | 1 mg SD i.v. (30 s bolus) | 8 | 0 | 21–32 | Not stated |
| PK study 10 ^a | Ref. 3 | 1 mg SD i.v. (1 h infusion) | 9 | 0 | 25–37 | Lanitor |
| PK study 11 ^a | Ref. 42 | 1 mg SD i.v. (30 s bolus) | 12 | 0 | NG | Lanoxin |
| PK study 12 ^b | Ref. 58 | 1 mg SD i.v. (30 min infusion) | 11 | 0 | 19–48 | Not stated |
| PK study 13 ^a | Ref. 3 | 1.5 mg SD i.v. (1 h infusion) | 9 | 0 | 25–37 | Lanitor |
| PK study 14 ^c | Ref. 33 | 0.25 mg SD p.o. | 16 | 0.31 | 18–45 | Glaxo Welcome |
| PK study 15 ^c | Ref. 59 | 0.5 mg SD p.o. | 10 | 0.9 | 19–25 | Orion, Espoo, Finland |
| PK study 16 ^c | Ref. 36 | 0.5 mg SD p.o. | 10 | 0 | 23–30 | Lanitor |
| PK study 17 ^c | Ref. 58 | 0.5 mg SD p.o. | 11 | 0 | 19–48 | Not stated |
| PK study 18 ^a | Ref. 44 | 0.5 mg SD p.o. | 12 | 0.42 | 19–35 | Nativelle |
| PK study 19 ^c | Ref. 35 | 0.5 mg SD p.o. | 12 | 0 | 21–31 | Lanitor |
| PK study 20 ^c | Ref. 60 | 0.5 mg SD p.o. | 12 | 0.08 | 22–35 | Nativelle |
| PK study 21 ^c | Ref. 34 | 0.5 mg SD p.o. | 18 | 0.44 | 19–36 | Nativelle |
| PK study 22 ^c | Ref. 41 | 0.75 mg SD p.o. | 12 | 0 | 21–39 | Lanitor |
| PK study 23 ^c | Ref. 61 | 1 mg SD p.o. | 5 | 0 | 23–32 | Lanoxin |
| PK study 24 ^a | Ref. 2 | 1 mg SD p.o. | 8 | 0 | 21–37 | Lanitor |
| PK study 25 ^c | Ref. 62 | 1 mg SD p.o. | 10 | 0 | 19–27 | Lanoxin |
| PK study 26 ^{d,e} | Ref. 63 | MD (0.125 mg q.d., 14 days) | 12 | 0 | 18–55 | Not stated |
| PK study 27 ^c | Refs. 64,65 | MD (0.25 mg q.d., 11 days) | 20 | 0.55 | 23–49 | Teofarma Srl |
| PK study 28 ^{d,e} | Ref. 66 | MD (0.25 mg q.d., 7 days) | 22 | 0.38 | 19–38 | Not stated |
| PK study 29 ^c | Ref. 45 | MD (0.5 mg, b.i.d., 3 days then 0.25 mg, b.i.d., 11 days) | 7 | 0 | 22–28 | Not stated |
| PK study 30 ^c | Ref. 67 | MD (0.25 mg b.i.d., 14 days) | 9 | 0 | 23–40 | Lanoxin |
| PK study 31 ^c | Ref. 67 | MD (0.25 mg b.i.d., 14 days) | 10 | 0 | 23–40 | Lanoxin |

SD, single dose; MD, multiple dose; NG, not given; i.v., intravenous.

The two oral studies in the training set were used only for the meta-analysis of renal clearance and to enable the assessment of the predicted k_a from the Mech P_{eff} model.

^aTrainings set ($n = 11$).

^bTest set ($n = 4$).

^cExternal validation set (16).

^dMajority blacks.

where $dA_{\text{diss},n}/dt$ is the dissolution rate, which can be either entered directly using measured *in vitro* profiles or calculated using a diffusion layer model.⁸ The term $dA_{\text{F},n}/dt$ indicates the release rate of solid drug from the formulation cases where this process is not immediate; $k_{\text{deg},n}$ and $k_{t,n}$, $k_{a,n}$ are drug degradation (luminal), segmental transit time and absorption rate constants; $CL_{\text{int-T},n}$ and $CL_{\text{int-G},n}$ are the net efflux clearance from the enterocyte and net metabolic clearance within the enterocyte, respectively; and $V_{\text{ent},n}$ and $Q_{\text{ent},n}$ are the volume of enterocytes in the segment and the blood flow to the segment, respectively.

The $P_{\text{app,Tran},n}$ value is then transferred to the corresponding *in vivo* effective active permeability values ($P_{\text{app,Tran},n}$) using the following equation for Caco-2 cells:

$$\log(P_{\text{eff,Tran},n}) = 0.6532 \times \log(P_{\text{app,Tran},n}) - 0.3036 \quad (6)$$

This $P_{\text{eff,Tran},n}$ value is scaled up to the transporter clearance in the n th gut segment, $CL_{\text{Tran},n}$, using the following equation:

$$\begin{aligned} CL_{\text{Tran},n}(\text{gut}) \\ = \text{REF}_{P\text{-gp}} \times P_{\text{eff,Tran},n} \times S_n \times \text{Transporter}_{\text{G,P-gp}} \end{aligned} \quad (7)$$

where S_n is the surface area of the gut segment and $\text{Transporter}_{\text{G,P-gp}}$ is the relative abundance of transporter (P-gp) in the gut segment, which is available within the Simcyp population library (details of the corresponding meta-analysis have been published recently¹⁰). The relative expression factor, REF, is the ratio of intestinal transporter abundance in the *Jejunum I* (per cm² of cylindrical surface area) versus that of the *in vitro* system (per cm²), where *Jejunum I* represents a segment of the ADAM model.¹⁰ This value can for instance be obtained by comparing relative abundances derived from Western blot studies or by comparison of absolute abundance data

from LC–MS/MS (liquid chromatography with tandem mass spectrometry) data. The REF can also be replaced by a RAF (relative activity factor), which would be more relevant. However, a REF and RAF can be used interchangeably, if the same activity is assumed per each transporter molecule *in vivo* and *in vitro*. Although this is a reasonable assumption for ATP-dependent transporters, this cannot be recommended for solute carriers, because these are generally dependent on counter ion gradients maintained by other solute carriers and hence sensitive to the environment in which they are located. An example is the Peptide transporter 1 (PepT1) the activity of which is linked to the sodium proton exchange 3 (NHE3).⁶⁸

The transporter abundance in each segment of the small intestine and the colon as a whole is expressed relative to the *Jejunum I* segment [transporter per cm² (relative values)]. The coefficient of variation (CV) for the intestinal transporter abundance (%) is expressed for *Jejunum I* only, but because the abundance for other gut segments are relative to *Jejunum I*, this CV is propagated to the other intestinal segments.¹⁰

Hepatic Transporters

A similar approach is adopted for *in vitro*–*in vivo* extrapolation of data relating to hepatic transporters. $J_{\max,i}$ (or $CL_{\text{int},i}$) is scaled to a whole liver value using the scaling factor (SF) defined below:

$$SF_i = \text{HPGL}_i \times \text{LiverWt}_i \times \text{REF}_i \times \text{CV}_i \times 60 \times 10^{-6} \quad (8)$$

where CV_i is the coefficient of variation for the *i*th transporter, REF_i is the relative expression factor for the *i*th transporter, HPGL_i is the inter-individual assigned value of hepatocyte per gram of liver, and LiverWt_i is the inter-individual assigned value for the liver weight. In this case, the REF is the ratio of the transporter abundance in human hepatocytes (per million cells) to that in the *in vitro* system, for example, Human Embryonic Kidney (HEK-293) cells (per million cells). Within the Simcyp Simulator, three apically localised efflux transporters, ABCB1 (P-gp), ABCC2 (MRP2) and ABCG2 (BCRP) are available. Information describing the variability in expression of each transporter across a healthy North European Caucasian population was collated from published data.¹⁰ Because the CL_{PD} entry unit is mL/min/millions of hepatocyte, the scaling factor for passive permeability ($SF_{\text{PD},i}$) across the hepatocyte is:

$$SF_{\text{PD},i} = \text{HPGL}_i \times \text{LiverWt}_i \times 60 \times 10^{-3} \quad (9)$$

It is worth noting that there is a difference between the SFs for the transporters and the passive membrane permeability.

Inhibition of P-gp-Mediated Efflux

A PBPK model accounting for competitive inhibition or induction of P-gp-mediated efflux can be used to simulate the effects of inhibitors or inducers on the intestinal and hepatic efflux of digoxin. The concentration of perpetrator at the binding site of P-gp, that is, the enterocyte concentration, $C_{\text{ent},n}$, in the *n*th segment, corrected for the free fraction ($f_{\text{u,gut}}$), is used for inhibition/induction of P-gp-mediated intestinal efflux of digoxin. The unbound (unionised and ionised) concentration of the perpetrator in the intracellular water of the liver ($C_{\text{IW,Liver}}$) is used for inhibition/induction of the canalicular efflux of digoxin.

Observed Pharmacokinetic Data for Digoxin

Thirty-one independent pharmacokinetic studies that evaluated digoxin were collated from the literature and used for model building (training set), model testing and verification (test set) and performance validation (external validation set). Details of these studies are given in Table 2.

Studies that were used for building the model are part of the training set—the parameters derived from these studies are listed in Table 1. The test set studies were used for model verification and consist of additional intravenous infusion and bolus studies not used in the model building stage. Finally, the external validation set consists of studies that involve oral dosing of digoxin over the entire clinically relevant dose range using both single and multiple dosing regimens.

Simulations

The sub-models and differential equations described above are components of the algorithms implemented within the Simcyp Population-Based Simulator (version 12.2; Simcyp Ltd., Sheffield, UK).¹³ The program allows facile extrapolation of *in vitro* enzyme kinetic data in both, liver and intestine, to predict pharmacokinetic changes *in vivo* in virtual populations. Genetic, physiological and demographic variables relevant to the prediction of drug–drug interactions are generated for each individual using correlated Monte Carlo methods and equations derived from population databases obtained from literature sources.⁶⁹

Studies Investigating the Impact of Dose on Digoxin Exposure

Simcyp (version 12.2) was used to simulate the time courses of digoxin concentrations in plasma. To

ensure that the characteristics of the virtual subjects were matched closely to those of the subjects studied *in vivo*, numbers, age range and gender ratios were replicated (Table 2). Twenty to forty separate trials were generated to assess variability across groups.

- Intravenous single dose studies: Twenty virtual trials of healthy volunteers (subject number, age range, percentage female according to Table 2) receiving a single intravenous bolus or infusion dose of 0.5, 0.75, 1 or 1.5 mg were generated. The simulated profiles for digoxin were compared with observed data from nine independent papers with 13 PK studies,^{2,3,37,40–42,56–58} respectively (Table 2).
- Single oral dose studies: Twenty virtual trials of healthy volunteers (subject number, age range, percentage female according to Table 2) receiving a single oral dose of 0.25, 0.5, 0.75 or 1 mg were generated. The simulated profiles for digoxin were compared with observed data from 12 independent PK studies,^{2,33–36,41,44,58–62} respectively (Table 2).
- Multiple dose studies: Twenty virtual trials of healthy volunteers (subject number, age range, percentage female according to Table 2) receiving either 0.125 mg digoxin (q.d., *quaque die* or “one a day”), 0.25 mg (q.d.), 0.25 mg (b.i.d.; *bis in die* or “twice a day”) or 0.5 mg (b.i.d.) were generated and the simulated profiles for digoxin were compared with those observed in six independent PK studies matching the dose regime simulated^{44,63–67,70} (Table 2).
- Inter-individual concentration–time profiles: Twenty virtual trials of 10 male subjects aged 23–30 years receiving a single oral dose of 0.5 mg digoxin were generated. The simulated individual profiles for digoxin were compared with observed data from Weiss *et al.*⁷¹ Forty virtual trials of five male subjects aged 23–32 years receiving a single oral dose of 1 mg digoxin were generated. The simulated individual profiles for digoxin were compared with observed data from Hayward *et al.* (1978).⁶¹

Simulation of Studies Investigating the Impact of P-gp Expression

Simulations were performed to investigate the impact of intestinal and hepatic P-gp abundance on the exposure to digoxin. This was carried out by changing the REF from 0.1 to 20. In addition, data relating to induction of intestinal P-gp by rifampicin were used to investigate the effects of this inducer on the systemic exposure of digoxin. Because concentration-dependent data relating rifampicin levels to P-gp induction were not available, the intestinal REF was

increased 3.5-fold to replicate the increase in expression observed after rifampicin treatment *in vivo*.² Although additional validations of the digoxin model with respect to inhibition of the P-gp-mediated efflux of digoxin have also been performed, these form the basis of another paper (Neuhoff *et al.*, 2013; Part II; accepted for publication in *Journal of Pharmaceutical Sciences*).

RESULTS

Concentration–Time Profiles Following a Single Dose of Digoxin

Predicted and observed plasma concentration–time profiles of digoxin after a single intravenous dose of 0.5, 0.75, 1 or 1.5 mg digoxin were compared for 20 virtual trials. In Figure 3, representative profiles for the best (a) and the worst (b) prediction overlay are shown. The individual simulated profiles for all 13 intravenous studies overlaid with the observed data are shown in the Supplementary Material I. Predicted and observed plasma concentration–time profiles of digoxin after a single oral dose of 0.25, 0.5, 0.75 or 1 mg digoxin in solution were also compared for 20 virtual trials. In Figure 3, representative profiles for the best (c) and the worst (d) prediction overlay are shown. The individual simulated profiles for all 12 oral studies overlaid with the observed data are also shown in the Supplementary Material I.

Following oral administration, the mean predicted area under the plasma concentration–time curve profiles ($AUC_{(0-\infty)}$) values of digoxin at 0.25 mg ranged from 10.03 to 13.43 ng/mL \times h for the 20 simulated trials (median 11.55) using male subjects between 20 and 50 years; the observed mean value was 17.05 ng/mL \times h.³³ Mean predicted $AUC_{(0-\infty)}$ values of digoxin at 0.5 mg ranged from 20.06 to 26.87 ng/mL \times h for the 20 simulated trials (median 23.1); the observed mean values were 36.7,⁶⁰ 28.3,³⁴ 18.4,⁵⁸ and 32.3 ng/mL \times h⁴⁴ (Table S1). Mean predicted $AUC_{(0-\infty)}$ values of digoxin at 0.75 mg ranged from 30.10 to 40.32 ng/mL \times h for the 20 simulated trials (median 34.65); the observed mean value was 14.9 ng/mL \times h.⁴¹ Mean predicted $AUC_{(0-\infty)}$ values of digoxin at 1 mg ranged from 40.13 to 53.76 ng/mL \times h for the 20 simulated trials (median 46.20); the observed mean values were 8.8 (reported only values for less than 7 h),² 61.9,⁶² 14.9 (reported only values for less than 7 h) ng/mL \times h,⁶¹ respectively (Table S2).

For an easy comparison between matched predictions for gender, age and dosing regimen and observed data, the ratio between predicted and observed maximum plasma concentration observed (C_{max}), time to maximum plasma concentration observed (t_{max}) and total clearance after intravenous and oral administration (CL_{iv} and CL_{po}) are presented (Figs. 4a–4d,

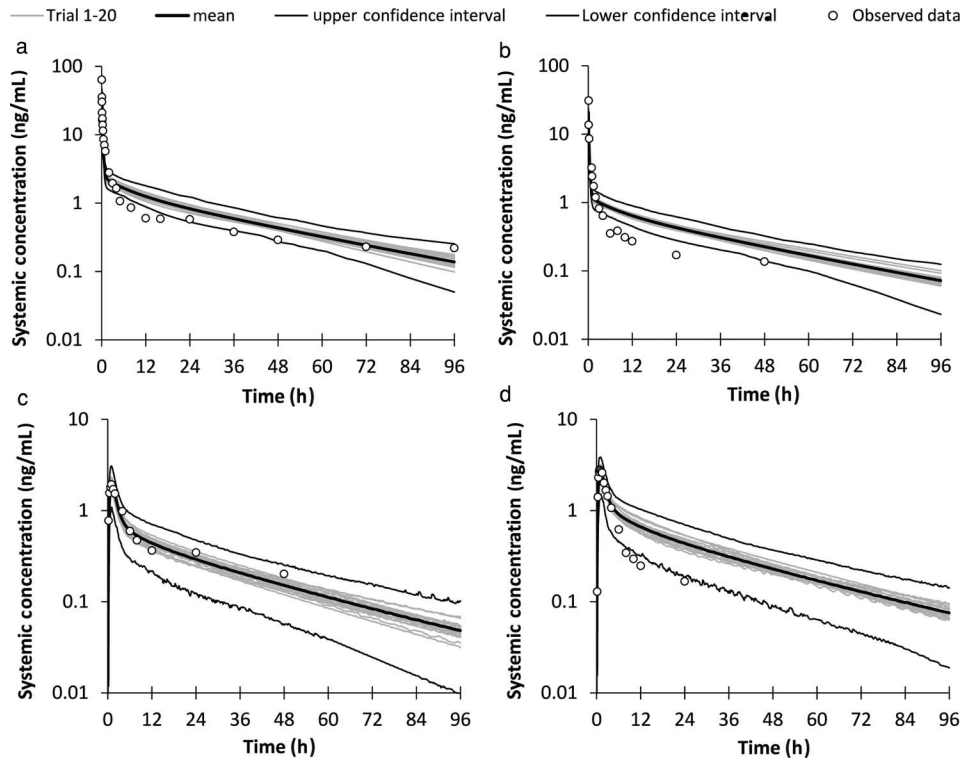


Figure 3. Predicted versus observed plasma concentration–time profiles of digoxin after a single intravenous bolus dose of (a) 1 mg⁴² and (b) 0.5 mg³⁷ or an oral dose of (c) 0.5 mg⁴⁴ and (d) 0.75 mg⁴¹, respectively. These are example of the performance verification for a (a and c) well-predicted and (b and d) the worst-predicted case. The grey lines represent 20 individual trials and the solid black line is the mean of the simulated population. Thin black lines are the 95th and 5th percentile predictions. Mean observed data are indicated by circles.

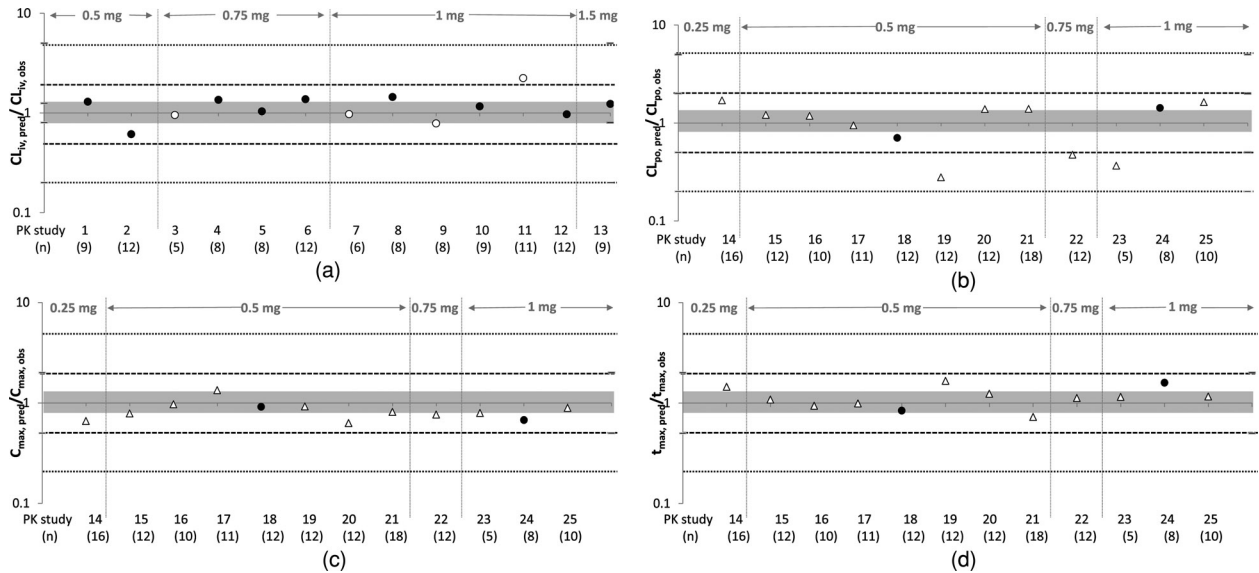


Figure 4. Goodness of the prediction: The model is judged based on calculated fold over- or under-prediction of the trainings set (filled circle), the test set (open circles) and the external validation set (open triangles). The ratio of the predicted and observed clearance of digoxin after a single intravenous dose (a) and the corresponding clearance (b), C_{max} (c) and t_{max} (d) ratios after oral dose are given within a 1.25-fold (grey area), twofold (dashed lines) and fivefold (dotted line) prediction range.

respectively). From the 13 intravenous studies, 12 were predicted within twofold of the observed values, independent of whether the study was used earlier in the model building process or part of an independent test set (Fig. 4a). Although a twofold change is generally accepted as an indicator of a good prediction, a twofold change in digoxin C_{\max} or AUC is cause for concern in the clinic, therefore, we evaluated a much narrower window of 1.25-fold.⁷² Ten of the 13 intravenous studies were also within the 1.25-fold prediction. From the 12 oral studies, only two were used for building the PBPK model, hence the remaining studies represented the external validation set. Of these 10 studies, five were within 1.25-fold, three were within twofold and two studies were within fivefold of the observed clearance. Among the latter, digoxin measurements were only collected up to 9³⁵ or 7 h after dosing,⁶¹ thus the reported AUC was low and the clearance high compared with those in the other reports evaluated here. Although C_{\max} ratios and t_{\max} ratios were all within the twofold range, generally the C_{\max} ratios were slightly under predicted (10 out of 12; Figs. 4c and 4d). Three-quarters of the C_{\max} ratios and two-thirds of the t_{\max} ratios were within 1.25-fold of the observed values.

Figures 5a and 5b show the simulated and observed individual plasma concentration–time profiles of digoxin after a single oral dose of 0.5 and 1 mg digoxin, respectively, based on the demographics (age, gender) and trial design from clinical studies.^{36,61,71} The simulated profiles are consistent with observed profiles which is also reflected in the C_{\max} and AUC ratios of 1.11 (2.14/1.93 ng/mL) and 1.10 (24.74/22.50 ng/mL × h) and 0.80 (3.81/4.74 ng/mL) and 0.77 (47.72/61.9 ng/mL × h) for 0.5 and 1 mg digoxin, respectively. A representative output of the simulated AUC values with corresponding estimated variability and comparable clinical data⁶¹ is shown in Figure 6.

When given alone, digoxin does not show a dose non-linearity, which is reflected by the constant dose-normalised, predicted C_{\max} (mean) values at different oral doses (Fig. 7); the 95th and 5th percentile range is based upon the study population reported (Table 2).

Concentration–Time Profiles During Chronic Oral Administration of Digoxin

Individual simulated profiles for all six multiple dose oral studies overlaid with the observed data are shown in the Supplementary Material I. Predicted and observed mean plasma concentration–time profiles of digoxin after 19 days of administration of 0.125 mg digoxin in solution (q.d.) were compared for 20 virtual trials. Mean predicted AUC_(0-∞) values of digoxin at 0.125 mg q.d. ranged from 6.34 to 7.66 ng/mL × h for the 20 simulated trials (median 6.95); the ob-

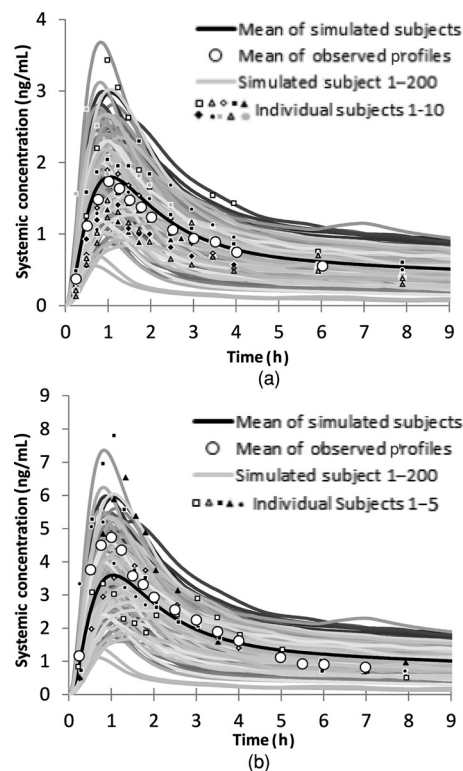


Figure 5. Simulated versus observed inter-individual plasma concentration–time profiles of digoxin (a) after a single oral dose of 0.5 mg digoxin. Twenty trials of 10 subjects were simulated based on trial design and age/sex of Weiss *et al.*⁷¹ and Westphal *et al.*³⁶ Thin grey lines represent the 200 simulated individuals; the small symbols indicate observed data points for 10 individuals⁷¹ and the open circles represent the observed mean data. (b) Represents corresponding data for a single oral dose of 1 mg digoxin. The thin grey lines are simulated data for 200 subjects; that is, 40 trials of five subjects, simulated based on trial design and age/sex of Hayward *et al.*⁶¹ The open circles indicate mean observed data points and the small symbols the individual data for the five individuals.⁶¹

served mean value was 6.96 ng/mL × h.⁶³ Digoxin was predicted to not accumulate over about 48 h during repeat dose administration of digoxin, with consistent maximum and minimum plasma concentrations thereafter (Table S3).

Predicted and observed mean plasma concentration–time profiles of digoxin after 8 days of administration of 0.25 mg digoxin in solution (q.d.) using the study design by Vaidyanathan *et al.*⁶⁶ were compared for 20 virtual trials in Figure 8. Mean predicted AUC_(0-∞) values of digoxin at 0.25 mg q.d. after 19 days ranged from 13.08 to 15.33 ng/mL × h for the 20 simulated trials (median 13.89); the observed mean value was 14.89 ng/mL × h⁶⁶ and 15.4 ng/mL × h⁶⁴ (Table S3).

Predicted and observed mean plasma concentration–time profiles of digoxin after 19 days of administration of 0.25 mg digoxin in solution (b.i.d.) were

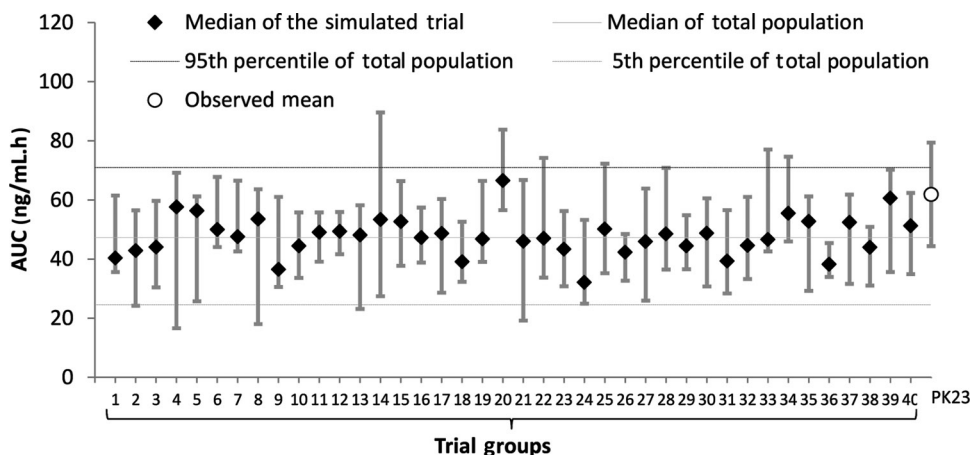


Figure 6. Median AUC values (5th and 95th percentiles) of digoxin after an oral dose of 0.5 mg digoxin in solution predicted in 40 different randomly selected groups of virtual subjects ($n = 5$; open circles) and observed (solid diamond) values. The solid line represents the median of the virtual population ($n = 200$); dashed lines represent the 5th and 95th percentiles of the virtual population. Trial group 41 indicates the observed data from Hayward *et al.*,⁶¹ that is, PK study Nr 23 in Table 2.

compared for 20 virtual trials. Mean predicted $AUC_{(0-\infty)}$ values of digoxin at 0.25 mg b.i.d. ranged from 11.83 to 16.64 ng/mL \times h for the 20 simulated trials (median 14.10); observed mean values were 10.16⁴⁵, 15.7⁶⁷ and 15.9 ng/mL \times h⁶⁷ (Table S3).

External Validations Using the Suppression and Induction Data

In Figure 9a, a sensitivity analysis on the REF value for intestinal P-gp is shown. The higher the REF value the greater the contribution of the efflux transporter, which has an obvious impact on C_{max} , that is, it causes a reduction. At an oral dose of 0.5 mg, a twofold increase in the REF from 2 to 4 leads to a reduction in the C_{max} from 1.5 to 1.2 ng/mL, whereas a fourfold increase reduces the C_{max} to 0.8 ng/mL. In contrast, reduced REF values of 0.4 and 0.1, lead to predicted

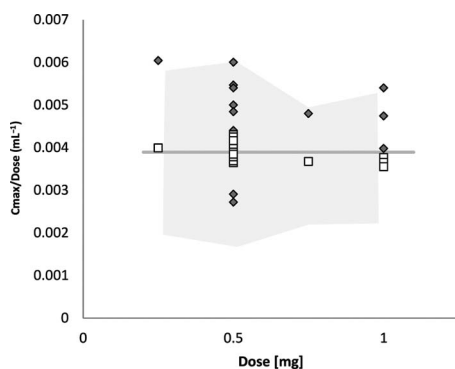


Figure 7. Sensitivity analysis on the linearity of the C_{max} , when normalised for dose. Simulated (open squares) and observed (grey diamonds) dose-normalised C_{max} values. The grey area represents the simulated 95th and 5th percentile of the virtual population matched to clinical studies.

increases in C_{max} values of 2 and 2.3 ng/mL, respectively. The observed range of mean C_{max} values after 0.5 mg oral dose digoxin are between 1.36⁵⁸ and 3 ng/mL.⁶⁰ Therefore, the default REF of 2 reflects the most contribution of P-gp within the observed range of C_{max} values and thus the worst case scenario for intestinal P-gp contribution to the absorption profile of digoxin.

Predicted decreases in $AUC_{(0-\infty)}$ and C_{max} of digoxin as a result of intestinal P-gp induction following administration of rifampicin (600 mg q.d. for 9 days) were 1.5- and 1.6-fold, which were broadly consistent with observed values of 1.4- and 2.2-fold, respectively.

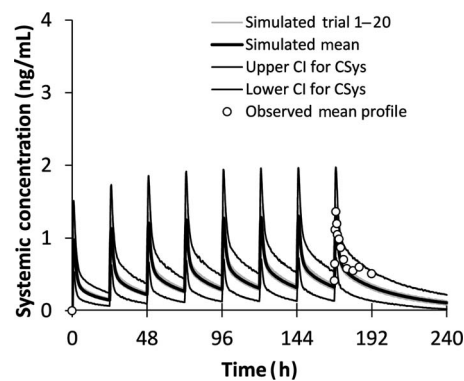


Figure 8. Predicted versus observed plasma concentration–time profile of digoxin after an oral dose of 0.25 mg q.d. during 8 days in a population of 220 individuals (20 trials of 22 healthy volunteers) age 19–38 years (0.38% female). The thin lines represent individual trials ($n = 20$) and the solid black line is the mean of the simulated population ($n = 220$). The open circles are mean observed values.^{64,65}

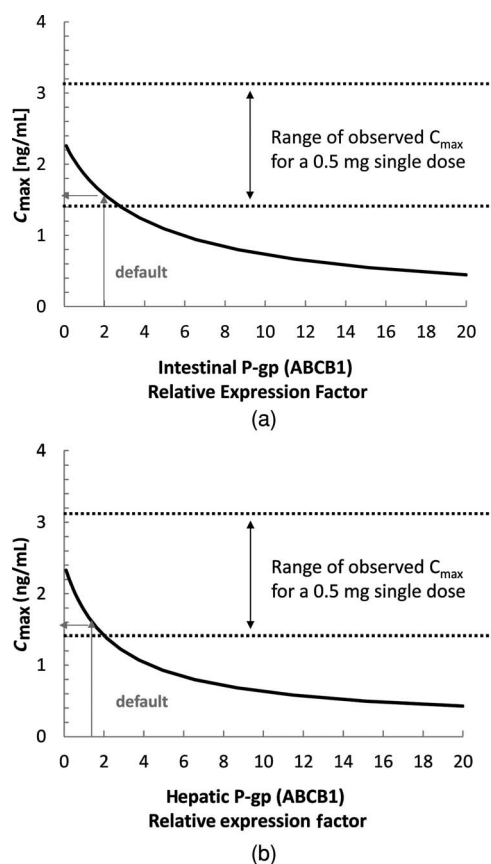


Figure 9. Sensitivity analysis on intestinal (a) and hepatic (b) REF of P-gp at a single oral dose of 0.5 mg. The range of observed C_{\max} for this dose is indicated between the two dotted lines. The grey arrows indicate the intestinal and hepatic REFs used for the current PBPK model for digoxin.

The impact of hepatic P-gp induction is shown in Figure 9b. At an oral dose of 0.5 mg, a twofold increase in the hepatic REF from 1.5 to 3 leads to a decrease in the C_{\max} from 1.5 to 1.1 ng/mL, whereas a fourfold increase decreases the C_{\max} to 0.85 ng/mL. In contrast, reduced REF values of 0.4 and 0.1, lead to predicted increases in C_{\max} values of 2.1 and 2.3 ng/mL, respectively. It is worth mentioning that induction of intestinal P-gp is more likely because of higher gut (enterocyte) concentration compared with the liver (hepatocyte).

DISCUSSION

Approximately half of currently marketed drugs are substrates, inhibitors or modifiers of P-gp,⁷³ thus providing an indication of the importance of P-gp in absorption, disposition, excretion and organ toxicity of drugs. It is becoming increasingly important to have interpretable *in vitro* assays and mathematical models that can describe the kinetics of P-gp substrates in addition to assessing related drug-drug interaction

potential during drug development. Although from a clinical standpoint, because of its narrow therapeutic window, digoxin can/should now be replaced by other drugs on the market, it remains a compound of interest. Digoxin is one of the few P-gp substrates that is known to be poorly metabolised and is “sensitive” to perpetrators of P-gp efflux, thus making it an ideal “*in vivo*” probe for investigation of P-gp-mediated interactions. Therefore, a PBPK model for digoxin that is capable of accounting for P-gp saturation, inhibition and induction/suppression is a useful tool in current drug development programs.

The model developed in this study was able to recover concentration–time profiles of digoxin that were consistent with observed data across 31 independent studies (13 intravenous single dose, 12 per oral single dose and six multiple dose studies). The results confirmed that there was no indication of a departure from dose proportionality over the oral dose range studied (0.25–1.5 mg), which is in agreement with the fact that digoxin is not a good inhibitor for P-gp but rather a substrate with a high K_m value.²³ Thus, digoxin itself does not saturate the transporter within the clinical dose range as reflected in the constant PK profiles. However, inhibitors and inducers of transporters can affect the PK profile of digoxin as indicated by the clinically relevant C_{\max} changes evaluated (Fig. 9).

The PBPK model of digoxin fulfilled generally the “twofold” criterion: however, digoxin has a narrow therapeutic window and so requires a more precise recovery of clinical data. Thus, a 1.25-fold prediction range was evaluated with the majority of simulations falling within this range. The studies that were not recovered by the model either reported incomplete concentration–time profiles or the formulation type was not stated, leaving the possibility that here were solubility/dissolution issues with these studies, factors currently not accounted for within our PBPK model. The latter aspect could be added to a refined model, although currently marketed formulations overcome the solubility and dissolution limitations of the drug on its own.

Studies with human liver slices indicate that digoxin uptake is due to both passive diffusion and active processes. Experiments with transfected cells (*e.g.* Chinese Hamster Ovary, HEK-293, Oocytes) and sandwich cultured human hepatocytes (SCHH) showed that digoxin is not transported by organic anion transporters (OAT1 and OAT2), organic cation transporters (OCT1 and OCT2), monocarboxylic transporter 8 (MCT8) or organic anionic transporting polypeptides (OATP1B1, OATP1B3 and OATP2B1),^{74–76} although digoxin has previously been considered to be an OATP1B3 substrate.⁷⁷ In humans, a sodium-independent, basolaterally expressed, organic solute transporter heterodimer (OST_{alpha/beta})

has been identified to efflux digoxin.⁷⁸ However, also at least one sodium-dependent uptake transporter⁷⁵ has been discussed for digoxin, and it is known that the overall transport of digoxin is H⁺-independent at least across Caco-2 cell monolayers.⁷⁹ Within the described PBPK model, a CL_{PD} value of 0.1 mL/min/10⁶ hepatocytes was assumed, which is in agreement with a high diffusion rate into hepatocytes and high intra-cellular accumulation of digoxin,^{76,80,81} thus accounting indirectly for the sinusoidal uptake and efflux transporters into the liver. If reliable *in vitro* data on the specific sinusoidal uptake and efflux transporter become available, these could easily be used to extend and refine the current PBPK model. However, the relative contributions of passive and active hepatic transport need to be refined and verified, as described here for the intestinal efflux component.

The pharmacokinetics of digoxin is only partly understood. There are data suggesting that liver clearance plays a relatively small role because less than 10% of the drug is excreted via the bile and digoxin is mainly found to be excreted unchanged in the urine. Also renal P-gp inhibition has been suggested as a cause for drug–drug interactions. Recently OATP4C1 (*SLCO4C1*) was identified in the kidney as a transporter putatively involved in tubular secretion of digoxin.⁸² It is noteworthy that OATP4C1 (OATP-H) is also expressed in the jejunum and liver⁴⁷ and that its membrane location in human is still unclear.⁸³ Renal excretion of digoxin seems to be largely mediated by glomerular filtration, but approximately one-third of the renal clearance can be assigned to the non-glomerular route.⁴¹ Therefore, it would be interesting to extend our PBPK model of digoxin to include P-gp-mediated luminal efflux and tubular secretion of digoxin, using the recently developed mechanistic kidney model (Mech KiM) within the Simcyp Simulator.⁸⁴

Several other, as yet unidentified, transporters are involved in the transport of digoxin. Apical efflux and basolateral uptake are essentially “working” in the same direction, but inhibition (saturation or induction) of one or the other may lead to very different effects, particularly for eliminating organs. Inhibition of the basolateral uptake transporter results in elevated digoxin exposure; that is, increased C_{\max} and/or AUC, whereas inhibition of P-gp increases, at least in the first instance, the concentration within the eliminating organ (hepatic or renal cells). However, inhibition and induction of the intestinal P-gp leads to increased and decreased C_{\max} and AUC respectively (Neuhoff *et al.*, 2013; Part II; accepted for publication in *Journal of Pharmaceutical Sciences*).

The PK parameters obtained from the digoxin PBPK model were sensitive to changes in levels of intestinal and hepatic efflux transporter within the system. These changes can represent transporter in-

hibition or induction indicating the capabilities of the model for the assessment of transporter-mediated drug–drug interactions.

CONCLUSION

PBPK modelling in conjunction with a mechanistic absorption model and reliable *in vitro* data on transporters can be used to assess the impact of dose on P-gp-mediated efflux and to elucidate the relative importance of intestinal and hepatic P-gp to the bioavailability of digoxin and other P-gp substrates.

Conflict of interest: Sibylle Neuhoff, Karen Rowland Yeo, Zoe Barter, Masoud Jamei and David Turner are employees in Simcyp Limited (a Certara Company). Amin Rostami-Hodjegan is an employee of the University of Manchester and part-time employee of Simcyp Limited (a Certara Company). Simcyp’s research is funded by a consortium of pharmaceutical companies.

ACKNOWLEDGMENTS

This work was funded by Simcyp Limited (a Certara Company). The Simcyp Simulator is freely available, following completion of the training workshop, to approved members of academic institutions and other non-for-profit organisations for research and teaching purposes. The help of James Kay and Emma Booker in preparing the manuscript is appreciated.

REFERENCES

1. Thiebaut F, Tsuruo T, Hamada H, Gottesman MM, Pastan I, Willingham MC. 1989. Immunohistochemical localization in normal tissues of different epitopes in the multidrug transport protein P170: Evidence for localization in brain capillaries and crossreactivity of one antibody with a muscle protein. *J Histochem Cytochem* 37(2):159–164.
2. Greiner B, Eichelbaum M, Fritz P, Kreichgauer HP, von Richter O, Zundler J, Kroemer HK. 1999. The role of intestinal P-glycoprotein in the interaction of digoxin and rifampin. *J Clin Invest* 104(2):147–153.
3. Ochs HR, Greenblatt DJ, Bodem G, Harmatz JS. 1978. Dose-independent pharmacokinetics of digoxin in humans. *Am Heart J* 96(4):507–511.
4. Terao T, Hisanaga E, Sai Y, Tamai I, Tsuji A. 1996. Active secretion of drugs from the small intestinal epithelium in rats by P-glycoprotein functioning as an absorption barrier. *J Pharm Pharmacol* 48(10):1083–1089.
5. Ma JD, Tsunoda SM, Bertino JS Jr, Trivedi M, Beale KK, Nafziger AN. 2010. Evaluation of *in vivo* P-glycoprotein phenotyping probes: A need for validation. *Clin Pharmacokinet* 49(4):223–237.
6. Park GD, Spector R, Goldberg MJ, Feldman RD. 1987. Digoxin toxicity in patients with high serum digoxin concentrations. *Am J Med Sci* 294(6):423–428.
7. Piergies AA, Worwag EM, Atkinson Jr AJ. 1994. A concurrent audit of high digoxin plasma levels. *Clin Pharmacol Ther* 55(3):353–358.
8. Jamei M, Turner D, Yang J, Neuhoff S, Polak S, Rostami-Hodjegan A, Tucker G. 2009. Population-based mechanistic

- prediction of oral drug absorption. *AAPS J* 11(2):225–237.
9. Darwich AS, Neuhoff S, Jamei M, Rostami-Hodjegan A. 2010. Interplay of metabolism and transport in determining oral drug absorption and gut wall metabolism: A simulation assessment using the “Advanced Dissolution, Absorption, Metabolism (ADAM)” model. *Curr Drug Metab* 11(9):716–729.
 10. Harwood MD, Neuhoff S, Carlson GL, Warhurst G, Rostami-Hodjegan A. 2012. Absolute abundance and function of intestinal drug transporters: A prerequisite for fully mechanistic in vitro–in vivo extrapolation of oral drug absorption. *Biopharm Drug Dispos* 34(1):2–28.
 11. Zhao P, Rowland M, Huang SM. 2012. Best practice in the use of physiologically based pharmacokinetic modeling and simulation to address clinical pharmacology regulatory questions. *Clin Pharmacol Ther* 92(1):17–20.
 12. Yu L, Gatlin L, Amidon G. 2000. Predicting oral drug absorption in humans. In *Transport processes in pharmaceutical systems*; Amidon G, Lee P, Eds. New York: Marcel Dekker, pp 377–409.
 13. Jamei M, Marciniak S, Feng K, Barnett A, Tucker G, Rostami-Hodjegan A. 2009. The Simcyp population-based ADME simulator. *Expert Opin Drug Metab Toxicol* 5(2):211–223.
 14. Tam D, Tirona RG, Pang KS. 2003. Segmental intestinal transporters and metabolic enzymes on intestinal drug absorption. *Drug Metab Dispos* 31(4):373–383.
 15. Cong D, Doherty M, Pang KS. 2000. A new physiologically based, segregated-flow model to explain route-dependent intestinal metabolism. *Drug Metab Dispos* 28(2):224–235.
 16. Ho S, Darwich AS, Jamei M, Rostami-Hodjegan A. In press. Advances in physiologically based modeling coupled with in vitro–in vivo extrapolation of ADMET: Assessing the impact of genetic variability in hepatic transporters. In *Encyclopedia of Toxicology*; Wexler P, Ed. 3rd ed. Amsterdam: Elsevier. (In press)
 17. Rodgers T, Leahy D, Rowland M. 2005. Physiologically based pharmacokinetic modeling 1: Predicting the tissue distribution of moderate-to-strong bases. *J Pharm Sci* 94(6):1259–1276.
 18. Rodgers T, Rowland M. 2006. Physiologically based pharmacokinetic modelling 2: Predicting the tissue distribution of acids, very weak bases, neutrals and zwitterions. *J Pharm Sci* 95(6):1238–1257.
 19. Rodgers T, Rowland M. 2007. Mechanistic approaches to volume of distribution predictions: Understanding the processes. *Pharm Res* 24(5):918–933.
 20. Andersson KE, Bertler A, Wettrell G. 1975. Post-mortem distribution and tissue concentrations of digoxin in infants and adults. *Acta Paediatr Scand* 64(3):497–504.
 21. Doherty JE, Perkins WH, Flanigan WJ. 1967. The distribution and concentration of tritiated digoxin in human tissues. *Ann Intern Med* 66(1):116–124.
 22. Karjalainen J, Ojala K, Reissell P. 1974. Tissue concentrations of digoxin in an autopsy material. *Acta Pharmacol Toxicol (Copenh)* 34(5):385–390.
 23. Troutman MD, Thakker DR. 2003. Efflux ratio cannot assess P-glycoprotein-mediated attenuation of absorptive transport: Asymmetric effect of P-glycoprotein on absorptive and secretory transport across Caco-2 cell monolayers. *Pharm Res* 20(8):1200–1209.
 24. Kalvass JC, Pollack GM. 2007. Kinetic considerations for the quantitative assessment of efflux activity and inhibition: Implications for understanding and predicting the effects of efflux inhibition. *Pharm Res* 24(2):265–276.
 25. Zamek-Gliszczynski MJ, Lee CA, Poirier A, Bentz J, Chu X, El-lens H, Ishikawa T, Jamei M, Kalvass JC, Nagar S, Pang KS, Korzekwa K, Swaan PW, Taub ME, Zhao P, Galetin A. ITC recommendations on transporter kinetic parameter estimation and translational modeling of transport-mediated PK and DDIs in humans. *Clin Pharmacol Ther* (In Press, epub date 2013/04/17).
 26. Ohnhaus EE, Dettli L, Spring P. 1972. Protein binding of digoxin in human serum. *Eur J Clin Pharmacol* 5:34–36.
 27. Hinderling PH, Hartmann D. 1991. Pharmacokinetics of digoxin and main metabolites/derivatives in healthy humans. *Ther Drug Monit* 13(5):381–401.
 28. Imawaka H, Ito K, Kitamura Y, Sugiyama K, Sugiyama Y. 2009. Prediction of human bioavailability from human oral administration data and animal pharmacokinetic data without data from intravenous administration of drugs in humans. *Pharm Res* 26(8):1881–1889.
 29. Obach RS, Lombardo F, Waters NJ. 2008. Trend analysis of a database of intravenous pharmacokinetic parameters in humans for 670 drug compounds. *Drug Metab Dispos* 36(7):1385–1405.
 30. Hinderling PH. 1984. Kinetics of partitioning and binding of digoxin and its analogues in the subcompartments of blood. *J Pharm Sci* 73(8):1042–1053.
 31. Cohnen E, Flasch H, Heinz N, Hempelmann FW. 1978. Partition coefficients and R_m -values of cardenolides (author’s transl). *Arzneimittelforschung* 28(12):2179–2182.
 32. Dzimir N, Fricke U, Klaus W. 1987. Influence of derivation on the lipophilicity and inhibitory actions of cardiac glycosides on myocardial $\text{Na}^+ - \text{K}^+$ -ATPase. *Br J Pharmacol* 91(1):31–38.
 33. Eckermann G, Lahu G, Nassr N, Bethke TD. 2012. Absence of pharmacokinetic interaction between roflumilast and digoxin in healthy adults. *J Clin Pharmacol* 52:251–257.
 34. Ragueneau I, Poirier JM, Radembo N, Sao AB, Funck-Brentano C, Jaillon P. 1999. Pharmacokinetic and pharmacodynamic drug interactions between digoxin and macrogol 4000, a laxative polymer, in healthy volunteers. *Br J Clin Pharmacol* 48(3):453–456.
 35. Tayrouz Y, Ding R, Burhenne J, Riedel KD, Weiss J, Hoppe-Tichy T, Haefeli WE, Mikus G. 2003. Pharmacokinetic and pharmacologic interaction between digoxin and Cremophor RH40. *Clin Pharmacol Ther* 73(5):397–405.
 36. Westphal K, Weinbrenner A, Giessmann T, Stuhr M, Franke G, Zschesche M, Oertel R, Terhaag B, Kroemer HK, Siegmund W. 2000. Oral bioavailability of digoxin is enhanced by talinolol: Evidence for involvement of intestinal P-glycoprotein. *Clin Pharmacol Ther* 68(1):6–12.
 37. Ding R, Tayrouz Y, Riedel KD, Burhenne J, Weiss J, Mikus G, Haefeli WE. 2004. Substantial pharmacokinetic interaction between digoxin and ritonavir in healthy volunteers. *Clin Pharmacol Ther* 76(1):73–84.
 38. Coltart J, Howard M, Chamberlain D. 1972. Myocardial and skeletal muscle concentrations of digoxin in patients on long-term therapy. *Br Med J* 2(5809):318–319.
 39. Wagner JG, Popat KD, Das SK, Sakmar E, Movahhed H. 1981. Evidence of nonlinearity in digoxin pharmacokinetics. *J Pharmacokinetic Biopharm* 9(2):147–166.
 40. Koup JR, Greenblatt DJ, Jusko WJ, Smith TW, Koch-Weser J. 1975. Pharmacokinetics of digoxin in normal subjects after intravenous bolus and infusion doses. *J Pharmacokinetic Biopharm* 3(3):181–192.
 41. Rengelshausen J, Goggelmann C, Burhenne J, Riedel KD, Ludwig J, Weiss J, Mikus G, Walter-Sack I, Haefeli WE. 2003. Contribution of increased oral bioavailability and reduced nonglomerular renal clearance of digoxin to the digoxin-clarithromycin interaction. *Br J Clin Pharmacol* 56(1):32–38.
 42. Kramer WG, Kolibash AJ, Lewis RP, Bathala MS, Visconti JA, Reuning RH. 1979. Pharmacokinetics of digoxin: Relationship between response intensity and predicted compartmental drug levels in man. *J Pharmacokinetic Biopharm* 7(1):47–61.

43. Sumner DJ, Russell AJ. 1976. Digoxin pharmacokinetics: Multicompartmental analysis and its clinical implications. *Br J Clin Pharmacol* 3(2):221–229.
44. Becquemont L, Verstuyft C, Kerb R, Brinkmann U, Lebot M, Jaillon P, Funck-Brentano C. 2001. Effect of grapefruit juice on digoxin pharmacokinetics in humans. *Clin Pharmacol Ther* 70(4):311–316.
45. Kirch W, Hutt HJ, Dylewicz P, Graf KJ, Ohnhaus EE. 1986. Dose-dependence of the nifedipine-digoxin interaction? *Clin Pharmacol Ther* 39(1):35–39.
46. Troutman MD, Thakker DR. 2003. Novel experimental parameters to quantify the modulation of absorptive and secretory transport of compounds by P-glycoprotein in cell culture models of intestinal epithelium. *Pharm Res* 20(8):1210–1224.
47. Hilgendorf C, Ahlin G, Seithel A, Artursson P, Ungell AL, Karlsson J. 2007. Expression of thirty-six drug transporter genes in human intestine, liver, kidney, and organotypic cell lines. *Drug Metab Dispos* 35(8):1333–1340.
48. Miki Y, Suzuki T, Tazawa C, Blumberg B, Sasano H. 2005. Steroid and xenobiotic receptor (SXR), cytochrome P450 3A4 and multidrug resistance gene 1 in human adult and fetal tissues. *Mol Cell Endocrinol* 231(1–2):75–85.
49. Nishimura M, Naito S. 2005. Tissue-specific mRNA expression profiles of human ATP-binding cassette and solute carrier transporter superfamilies. *Drug Metab Pharmacokinet* 20(6):452–477.
50. von Richter O. 2000. Expression und Funktion arzneimittelmetabolisierender Enzyme und des ABC-Transporters P-Glykoprotein in Dünndarm und Leber des Menschen. Department of chemistry and pharmacy, Tübingen: Eberhard-Karls-Universität Tübingen.
51. Johnson TN, Tucker GT, Tanner MS, Rostami-Hodjegan A. 2005. Changes in liver volume from birth to adulthood: A meta-analysis. *Liver Transpl* 11(12):1481–1493.
52. Barter ZE, Chowdry JE, Harlow JR, Snawder JE, Lipscomb JC, Rostami-Hodjegan A. 2008. Covariation of human microsomal protein per gram of liver with age: Absence of influence of operator and sample storage may justify interlaboratory data pooling. *Drug Metab Dispos* 36(12):2405–2409.
53. Oliver RE, Jones AF, Rowland M. 1998. What surface of the intestinal epithelium is effectively available to permeating drugs? *J Pharm Sci* 87(5):634–639.
54. Pade D, Turner D, Jamei M, Antonovic L, Martinez M, Rostami-Hodjegan A. 2011. A performance evaluation of Simcyp Dog—A fully mechanistic physiologically based pharmacokinetic dog model based upon a variety of celecoxib IV and oral formulations. In *AAPS Annual Meeting*; Washington, D.C.
55. Amidon GL, Lennernas H, Shah VP, Crison JR. 1995. A theoretical basis for a biopharmaceutic drug classification: The correlation of in vitro drug product dissolution and in vivo bioavailability. *Pharm Res* 12(3):413–420.
56. Hager WD, Fenster P, Mayersohn M, Perrier D, Graves P, Marcus FI, Goldman S. 1979. Digoxin-quinidine interaction pharmacokinetic evaluation. *N Engl J Med* 300(22):1238–1241.
57. Pedersen KE, Dorph-Pedersen A, Hvidt S, Klitgaard NA, Nielsen-Kudsk F. 1981. Digoxin-verapamil interaction. *Clin Pharmacol Ther* 30(3):311–316.
58. Reitman ML, Chu X, Cai X, Yabut J, Venkatasubramanian R, Zajic S, Stone JA, Ding Y, Witter R, Gibson C, Roupe K, Evers R, Wagner JA, Stoch A. 2011. Rifampin's acute inhibitory and chronic inductive drug interactions: Experimental and model-based approaches to drug-drug interaction trial design. *Clin Pharmacol Ther* 89(2):234–242.
59. Jalava KM, Partanen J, Neuvonen PJ. 1997. Itraconazole decreases renal clearance of digoxin. *Ther Drug Monit* 19(6):609–613.
60. Verstuyft C, Strabach S, El-Morabet H, Kerb R, Brinkmann U, Dubert L, Jaillon P, Funck-Brentano C, Trugnan G, Becquemont L. 2003. Dipyrindamole enhances digoxin bioavailability via P-glycoprotein inhibition. *Clin Pharmacol Ther* 73(1):51–60.
61. Hayward RP, Greenwood H, Hamer J. 1978. Comparison of digoxin and medigoxin in normal subjects. *Br J Clin Pharmacol* 6(1):81–86.
62. Oosterhuis B, Jonkman JH, Andersson T, Zuiderwijk PB, Jedema JN. 1991. Minor effect of multiple dose omeprazole on the pharmacokinetics of digoxin after a single oral dose. *Br J Clin Pharmacol* 32(5):569–572.
63. Qiu R, Plowchalk DR, Byon W, Terra SG, Corrigan B, Mordenti J, Fang J, Fullerton T. 2010. Lack of a pharmacokinetic interaction between dimebon (latrepirdine) and digoxin in healthy subjects. *Clin Pharmacol Ther* 87(S1):S91: PIII–72.
64. Friedrich C, Ring A, Brand T, Sennewald R, Graefe-Mody U, Woerle H-J. 2010. Linagliptin has no pharmacokinetic interactions with digoxin in healthy volunteers. *Clin Pharmacol Ther* 87(S1):S31: PI–69.
65. Friedrich C, Ring A, Brand T, Sennewald R, Graefe-Mody EU, Woerle HJ. 2011. Evaluation of the pharmacokinetic interaction after multiple oral doses of linagliptin and digoxin in healthy volunteers. *Eur J Drug Metab Pharmacokinet* 36(1):17–24.
66. Vaidyanathan S, Camenisch G, Schuetz H, Reynolds C, Yeh CM, Bizot MN, Dieterich HA, Howard D, Dole WP. 2008. Pharmacokinetics of the oral direct renin inhibitor aliskiren in combination with digoxin, atorvastatin, and ketoconazole in healthy subjects: The role of P-glycoprotein in the disposition of aliskiren. *J Clin Pharmacol* 48(11):1323–1338.
67. Rodin SM, Johnson BF, Wilson J, Ritchie P, Johnson J. 1988. Comparative effects of verapamil and isradipine on steady-state digoxin kinetics. *Clin Pharmacol Ther* 43(6):668–672.
68. Watanabe C, Kato Y, Ito S, Kubo Y, Sai Y, Tsuji A. 2005. Na⁺/H⁺ exchanger 3 affects transport property of H⁺/oligopeptide transporter 1. *Drug Metab Pharmacokinet* 20(6):443–451.
69. Howgate EM, Rowland Yeo K, Proctor NJ, Tucker GT, Rostami-Hodjegan A. 2006. Prediction of in vivo drug clearance from in vitro data. I: Impact of inter-individual variability. *Xenobiotica* 36(6):473–497.
70. Rodin SM, Johnson BF. 1988. Pharmacokinetic interactions with digoxin. *Clin Pharmacokinet* 15(4):227–244.
71. Weiss M, Li P, Roberts MS. 2010. An improved nonlinear model describing the hepatic pharmacokinetics of digoxin: Evidence for two functionally different uptake systems and saturable binding. *Pharm Res* 27(9):1999–2007.
72. Fenner KS, Troutman MD, Kempshall S, Cook JA, Ware JA, Smith DA, Lee CA. 2009. Drug-drug interactions mediated through P-glycoprotein: Clinical relevance and in vitro-in vivo correlation using digoxin as a probe drug. *Clin Pharmacol Ther* 85(2):173–181.
73. Sedykh A, Fourches D, Duan J, Hucke O, Garneau M, Zhu H, Bonneau P, Tropsha A. 2013. Human intestinal transporter database: QSAR modeling and virtual profiling of drug uptake, efflux and interactions. *Pharm Res* 30(4):996–1007.
74. Kimoto E, Chupka J, Xiao Y, Bi YA, Duignan DB. 2011. Characterization of digoxin uptake in sandwich-cultured human hepatocytes. *Drug Metab Dispos* 39(1):47–53.
75. Acharya P, O'Connor MP, Polli JW, Ayrton A, Ellens H, Bentz J. 2008. Kinetic identification of membrane transporters that assist P-glycoprotein-mediated transport of digoxin and loperamide through a confluent monolayer of MDCKII-hMDR1 cells. *Drug Metab Dispos* 36(2):452–460.
76. De Bruyn T, Ye ZW, Peeters A, Sahi J, Baes M, Augustijns PF, Annaert PP. 2011. Determination of OATP-, NTCP- and OCT-mediated substrate uptake activities in individual and pooled

- batches of cryopreserved human hepatocytes. *Eur J Pharm Sci* 43(4):297–307.
77. Kullak-Ublick GA, Ismail MG, Stieger B, Landmann L, Huber R, Pizzagalli F, Fattinger K, Meier PJ, Hagenbuch B. 2001. Organic anion-transporting polypeptide B (OATP-B) and its functional comparison with three other OATPs of human liver. *Gastroenterology* 120(2):525–533.
78. Seward DJ, Koh AS, Boyer JL, Ballatori N. 2003. Functional complementation between a novel mammalian polygenic transport complex and an evolutionarily ancient organic solute transporter, OSTalpha-OSTbeta. *J Biol Chem* 278(30):27473–27482.
79. Neuhoff S, Ungell AL, Zamora I, Artursson P. 2003. pH-Dependent bidirectional transport of weakly basic drugs across Caco-2 monolayers: Implications for drug-drug interactions. *Pharm Res* 20(8):1141–1148.
80. Olinga P, Merema M, Hof IH, Slooff MJ, Proost JH, Meijer DK, Groothuis GM. 1998. Characterization of the uptake of rocuronium and digoxin in human hepatocytes: Carrier specificity and comparison with in vivo data. *J Pharmacol Exp Ther* 285(2):506–510.
81. Bi YA, Kazolias D, Duignan DB. 2006. Use of cryopreserved human hepatocytes in sandwich culture to measure hepatobiliary transport. *Drug Metab Dispos* 34(9):1658–1665.
82. Mikkaichi T, Suzuki T, Onogawa T, Tanemoto M, Mizutamari H, Okada M, Chaki T, Masuda S, Tokui T, Eto N, Abe M, Satoh F, Unno M, Hishinuma T, Inui K, Ito S, Goto J, Abe T. 2004. Isolation and characterization of a digoxin transporter and its rat homologue expressed in the kidney. *Proc Natl Acad Sci U S A* 101(10):3569–3574.
83. Kuo KL, Zhu H, McNamara PJ, Leggas M. 2012. Localization and functional characterization of the rat Oatp4c1 transporter in an *in vitro* cell system and rat tissues. *PLoS One* 7(6):e39641.
84. Neuhoff S, Gaohua L, Burt H, Jamei M, Li L, Tucker GT, Rostami-Hodjegan A. in press. Accounting for transporters in renal clearance: Towards a mechanistic kidney model (Mech KiM). In *Transporters in drug discovery, development and use*; Steffansen B, Sugiyama Y, Ed. New York: Springer. (in press)